SDC-92-222

SDC
SOLENOIDAL DETECTOR NOTES

FINITE ELEMENT ANALYSIS OF THE SDC BARREL AND ENDCAP CALORIMETERS

March 11, 1992

V. Guarino, N. Hill and J. Nasiakta
Argonne National Laboratory

In designing the SDC barrel and endcap calorimeters, the inter-module connecting forces must be known in order to determine the required size and number of connecting links between modules, and in order to understand how individual modules will be affected by these forces when assembled to form a full barrel and endcap. The connecting forces were found by analyzing three-dimensional Finite Element Models of both the barrel and endcap. This paper is divided into two parts, the first part will describe in detail the results of the barrel analysis and the second part will describe the results obtained from the endcap analysis. A similar approach was used in constructing the models for both analysis.

The ANL Model B cross section, dated September 10, 1991, was used as the base design. This design called for a lead HAD1 section in both the barrel and endcap. This design has subsequently been changed to an all-steel HAD1 in both the barrel and endcap. In both cases, an individual module, which approximates the stiffness of the EM, HAD1 and HAD2 sections and includes the outside radius structural iron, was first modeled. This simplified model of the individual wedge modules was then used in order to reduce the size of the problem and to reduce the amount of computer time required. An exact model of the individual modules would have been too large to run, but it was felt that an accurate prediction of the connecting forces could be found by using a simplified model as long as it was able to approximate the stiffness and weight distribution of the modules.

The EM, HAD1 and HAD2 sections of the barrel were modeled using solid elements when, in reality, they are laminated structures and therefore do not have the same stiffness as solid materials. The composite stiffness used to model these sections was found by using the ratio of the load carrying area of a cell to the total cell area and multiplying it by the stiffness of solid lead in the case of the EM and HAD1 sections. The density was also modified appropriately throughout the modules. The endcap was modeled using plate elements for the EM and HAD1 sections, and solid elements for the HAD2 section. However, to reduce the problem size, the number of plates were reduced, but the corresponding thicknesses were then increased to keep the mass and weight distribution the same. These modules were then copied and rotated to form the full barrel or endcap. Each module was separated by approximately .030 inches and connected by stiff beam elements at 15 points in the barrel and 22 points in the endcap.

Once the connecting forces acting between modules and the displacement of individual nodes are fully compiled using these simplified models of the barrel and endcap modules, they will be applied to a detailed model of each module to determine the internal stresses and deflections which can be expected.

Barrel Analysis

The barrel module was created by first modeling the endplates, the EM front plate, the plate at the EM-HAD1 boundary, the plate at the HAD1-HAD2 boundary and the outside radius structural iron with plate elements to form the structural frame as shown in Figure 1. All of the plates were given their appropriate thicknesses. The space between the plates was then filled with solid elements which were given the appropriate stiffness and density to approximate the EM, HAD1 and HAD2 sections. The connections between the modules were made at the EM-HAD1 boundary, the HAD1-HAD2 boundary and along the outside radius iron. Figure 2 shows the completed module with the location of the connecting nodes. The modules were connected together using beam elements which were modeled as circular rods. Each module was then copied and integrated into the model to form the quarter barrel shown in Figure 3. The modules were numbered from the top with the module in the 12 o'clock position assigned position one and then each module added in a clockwise direction when looking toward the interaction point along the beam axis from the endcap. Only a quarter barrel is needed for the analysis since symmetry produces duplicate results.

The barrel was supported at the bottom in an arc of 45° which resulted in the bottom 8 modules being supported along the entire length of their back iron. The bottom support was assumed to be completely rigid. All of the modules were restrained from moving in the beam direction at the $z = 0$ plane. It was assumed that the two half barrels would be connected at $z = 0$ in the final assembly and therefore they would be prevented from moving in the beam direction.

The EM, HAD1 and HAD2 sections are layered structures that have been approximated by solid elements. The stiffness of these sections is unknown and must be approximated. The HAD2 section is a welded structure with alternating cells, therefore it was felt that the modulus of steel, 30×10^6 psi, would be a good approximation of the HAD2 stiffness. The HAD1 and EM sections however are composed of layers of lead connected together with thin (.020") bulkheads. The stiffness of these structures obviously

is much lower than that of solid lead, however it is impossible to approximate accurately the stiffness of the two sections. In order to accomplish this, it was reasoned that by establishing upper and lower boundary conditions, the extreme limits of the problem would be established. The upper limit of the stiffness of these sections is the modulus of solid lead, the lower limit was found by taking the ratio of the load carrying area to the area of a cell (the bulkhead area) to the total area of a cell and multiplying it by the modulus of lead. Separate cases of the analysis were then run using these upper and lower limits of the EM and HAD1 stiffness. This method will not allow exact values of the connecting forces to be calculated, however we will be able to bound these forces and then design for the maximum possible.

Four different cases were run using a combination of stiffnesses for the EM and HAC1 sections and using different size rods to connect the modules together. The cases are summarized below:

Case #	*EM Stiffness (psi)*	*HAD1 Stiffness (psi)*	*Rod. Diameter (inches)*
1	2×10^6	2×10^6	1/4
2	24×10^3	35×10^3	1/4
3	2×10^6	2×10^6	1
4	24×10^3	35×10^3	1

The connecting forces calculated for the barrel are forces which are distributed along the length of the boundary plates. For example if a maximum normal connecting force of 400,000 lbs. is found along the EM-HAD1 boundary and this boundary has 29 bearing points at which the modules are connected and each point has a cross sectional area of 1 square inch then each point carries of load of ≈ 14,000 lbs. and has a stress of 14,000 psi.

The normal forces between modules at the EM-HAD1 boundary are shown in Figure 4. The normal force is plotted as a function of module position in the barrel. It can be seen in Figure 4 that cases 1 and 3, which differ only by the size of the rod, and case 2 and 4, which also only differ by the size of the connecting rod closely follow each other. Therefore the size of the connecting rod has no affect on the normal force. The maximum compression force ranges from 100,000 lbs. which occurred when the lower stiffness values were used and 290,000 lbs. which occurred when the upper limit of the stiffnesses

was used. The maximum tensile force of 110,000 lbs. occurs when the upper limit of the stiffnesses are used as compared to a tensile force of 80,000 lbs. when the lower limit of the stiffnesses are used. The normal force drops to approximately zero for the last eight modules since these are fixed to an assumed rigid cradle.

Figure 5 shows the normal force along the HAD1-HAD2 boundary as a function of module position in the barrel. Once again Case 1 and 3 closely follow each other and Case 2 and 4 follow each other. The only difference between Case 1 and 3 and Case 2 and 4 is the size of the connecting rod, therefore, size of the connecting rod has no affect on the normal force between modules. The maximum tensile force is 200,000 lbs. and occurs when the lower stiffness is used and compares to a tensile force of 100,000 lbs. when the upper limit stiffness is used. The maximum compression force of 600,000 lbs. occurs with the lower limit of the stiffness and a compression force of only 400,000 lbs. occurs when the upper limit stiffnesses are used. Once again the connecting forces drop to approximately zero for the last 8 modules which are supported by the cradle.

Figure 6 shows the normal connecting force along the outer radius structural iron as a function of module position in the barrel. Once again cases 1 and 3 and cases 2 and 4 follow each other exactly showing that the size of the connecting rod has no affect on the magnitude of the connecting forces. The maximum compressive force is 800,000 lbs. which occurs when the lower limit of the stiffnesses are used and a force of 780,000 lbs. occurs when the upper limit of the stiffnesses is used. The forces are reduced to zero for the last eight modules because they are fully supported along the back by the cradle.

Figure 7 through 9 show the shear forces in the radial direction for cases 1 and 4. Case 2 results are approximately the same as Case 4, and Case 3 results are approximately the same as Case 1, so they are not shown. A negative value of the radial force indicates a force pointing inward toward the beam line. Figure 7 shows the radial shear force along the EM-HAD1 boundary as a function of module position in the barrel. The maximum negative radial force is 7,000 lbs. and occurs when the upper limit of the stiffness is used and the maximum positive radial force is 15,000 lbs. and also occurs when the upper limit of the stiffnesses is used. Figure 8 shows the radial shear force along the HAD1-HAD2 boundary as a function of the module position around the barrel. The maximum positive radial shear force is 22,000 lbs., and the maximum negative radial shear force is 62,000 lbs. They both occur when the lower limit of the stiffnesses are used. Figure 9 shows the radial shear force along the back iron as a function of module position around the barrel.

The maximum positive radial shear force is 50,000 lbs. and the maximum negative radial shear force is 250,000 lbs. and both occur when the lower limit of the stiffnesses are used.

Figures 10 through 12 show the shear forces in the beam direction. A positive value of the z shear force is a force in the direction of the beam. Figure 10 shows the z direction shear force along the EM-HAD1 boundary as a function of the module position around the barrel. The maximum negative z shear force is 12,000 lbs. and the maximum positive z shear force is 34,000 lbs. and both occur when the upper limit case for stiffness is used. Figure 11 shows the z direction shear force along the HAD1-HAD2 boundary as a function of the module position in the barrel. The maximum negative force is 18,000 lbs. and the maximum positive force is 48,000 lbs. and both occur when the lower limit case for stiffness is used. Figure 12 shows the z direction shear force along the outside iron as a function of module position in the barrel. The maximum negative force is 18,000 lbs. and the maximum positive force is 36,000 lbs. and both occur when the lower limit of the stiffness is used.

Figure 13 shows the vertical deflection of the Barrel at the outside diameter for the four Cases analyzed. The maximum deflection for all of the cases is approximately .5 mm and it then decreases to zero for the last eight modules where the cradle begins.

Endcap Analysis

The endcap was modeled in a manner similar to that of the barrel. The EM front plate, the EM-HAD1 boundary plate, HAD1-HAD2 boundary plate and the back iron structure were modeled first using plate elements with the appropriate thicknesses to form the basic frame as shown in Figure 14. The individual modules were connected to each other at 22 points, 8 along the EM-HAD1 boundary, 6 along the HAD1-HAD2 boundary and 8 along the back iron. The EM and HAD1 sections, once again, are composed of layers of lead plates separated by thin bulkheads. This presents the same problem for modeling as it did in the barrel, how to model the stiffness of these structures appropriately while keeping the size of the problem manageable?

Instead of modeling the EM and HAD1 structures using solid elements and then varying the stiffnesses of this solid to approximate the stiffness of the structures to approximate the stiffness of the structures, a slightly different approach was taken. A reduced number of individual plates with correspondingly increased thickness were used.

The EM section has 12 lead plates 10.5 mm thick separated by bulkheads, these were approximated by 4 plates which were 1.24" thick and separated by 7 bulkheads. This method approximates the stiffness of the EM structure but does not go into so much detail that the problem becomes to large to run. Similarly the HAD1 section has 28 steel plates 20.5 mm thick which were approximated by 5 plates that are 4.5" thick and separated by 9 bulkheads. The stiffness of lead (2×10^6 psi) was used for the EM1 and the stiffness of steel (30×10^6 psi) was used for the HAD1 and bulkheads. The HAD2 section was approximated by solid elements and a modified stiffness (27×10^6 psi). Since HAD2 is a welded structure with very few gaps, it was felt that it would behave almost like a solid structure. Figure 15 shows the module wedge and the position of the connecting points. This module was then copied and rotated to form a half endcap as shown in Figure 16. Advantage was taken of symmetry so that only half of the endcap was modeled which reduced the size of the problem and computer time considerably. The bottom 4 modules (45°) were fully supported along the entire length of the outside diameter of the structural iron.

The connecting forces, as a function of module position in the endcap, are shown in Figs. 17-25. Because the connecting boundaries increase radially, each individual point was plotted, rather than a summation at each boundary. Figures 17-19 show the normal forces across the EM/HAD1, HAD1/HAD2, and outer iron (bending HAD2) boundaries, respectively. These forces range from zero at the first module to a maximum compressive load of 18,000 lbs. at the EM/HAD2, 30,000 lbs. at the HAD1/HAD2, and 32,000 lbs. at the outer iron boundaries.

The radial shear forces are shown in Figs. 20-22. These forces range from -2,500 lbs. to 7,500 lbs at the EM/HAD2 boundary, and from -12,000 lbs. to 17,000 lbs. at the outer iron. A negative force indicates a radially inward (towards the beam line) tendency. The z direction shear forces are shown in Figs. 23-25. These forces are very small, ranging from -11,000 lbs. to 2,000 lbs.

Summary

In summary, if one accepts the parameters that were used to establish stiffness of the models, the results indicate a totally feasible design. The maximum forces indicated at any boundary are well within the design capabilities in terms of being able to deal with them. As an example, in support of this premise one can refer to Fig. 6. The maximum

total force normal to the surface of the outside structural iron flange is indicated at ≈ 800,000 lbs. compression. The total surface area available to support this load is, according to current design, set at a range from ≈ 56 in.^{2} to 580 in^2 depending on how the iron structure is utilized. At these extremes, the respective compressive stresses are well within acceptable limits for steel, where compressive stress at yield of low carbon steel is accepted at 36,000 psi. Other boundaries have similar characteristics as shown in Figs. 4 and 5. Tension loads, although more difficult to deal with, are also within acceptable limits.

Work supported by the U.S. Department of Energy, Division of High Energy Physics, under contract W-31-109-ENG-38.

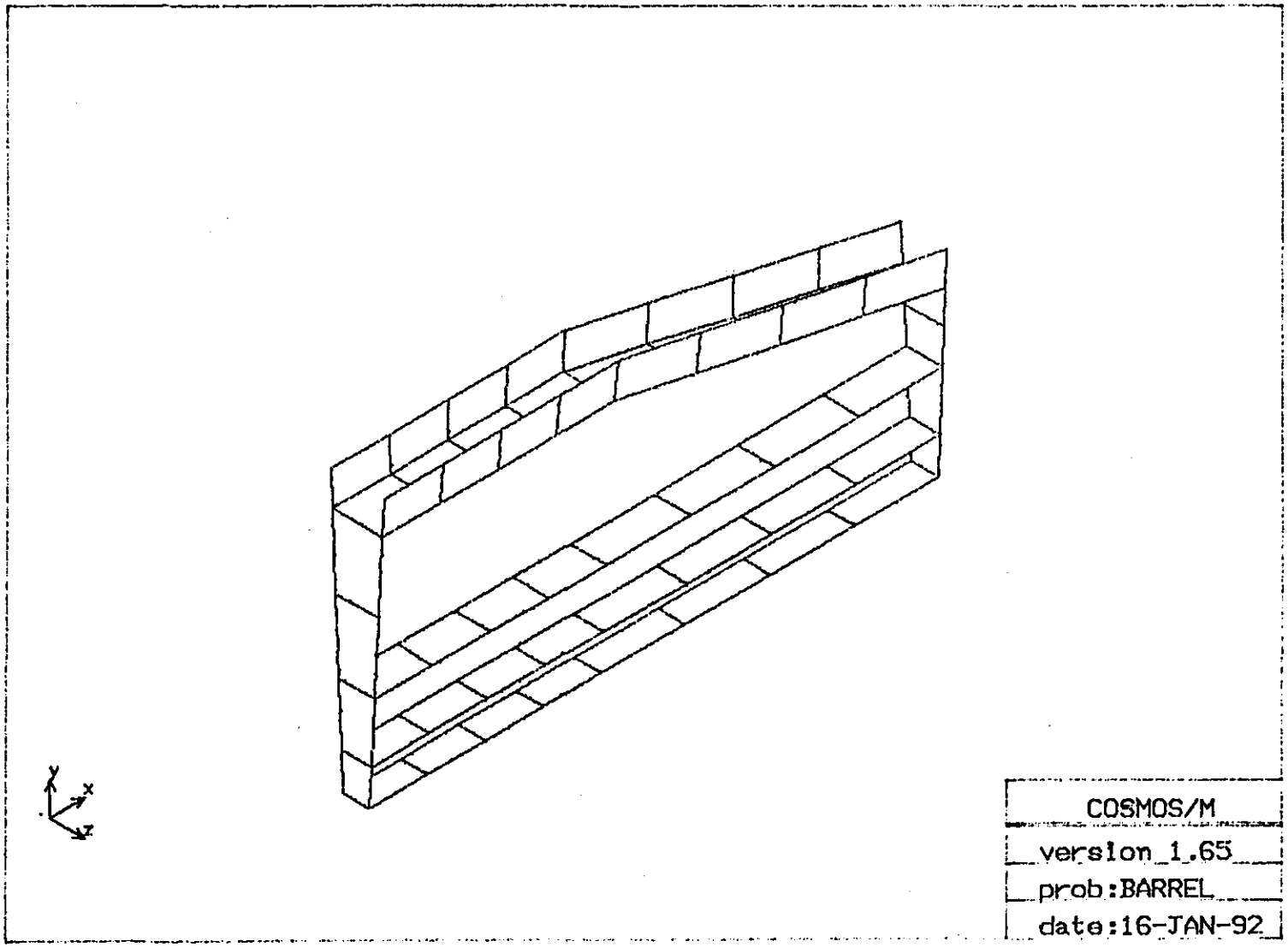

Figure 1

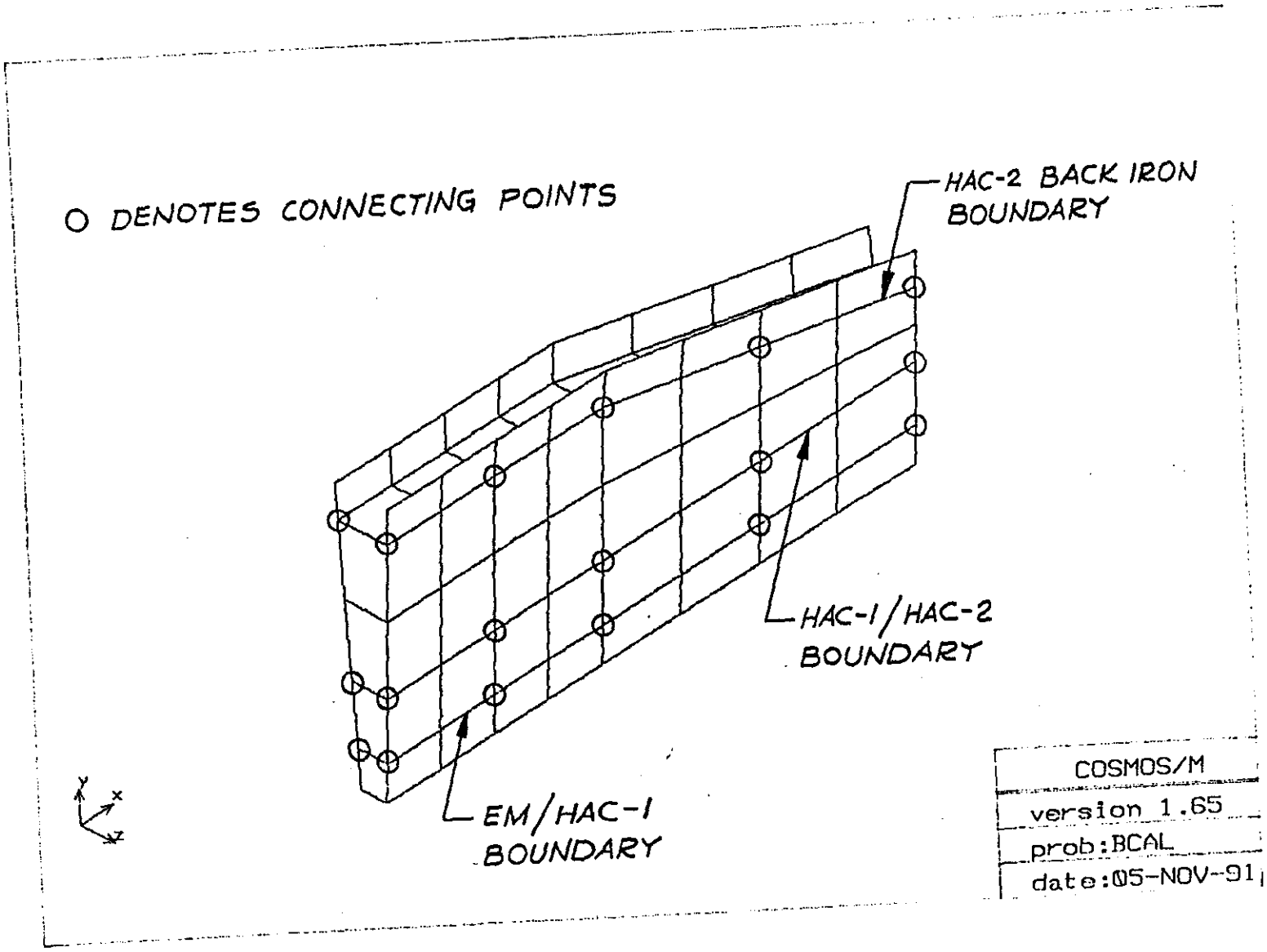
O DENOTES CONNECTING POINTS
HAC-2 BACK IRON BOUNDARY
HAC-1/HAC-2 BOUNDARY
EM/HAC-1 BOUNDARY
Y
X
Z
COSMOS/M
version 1.65
prob:BCAL
date:05-NOV-91

Figure 2

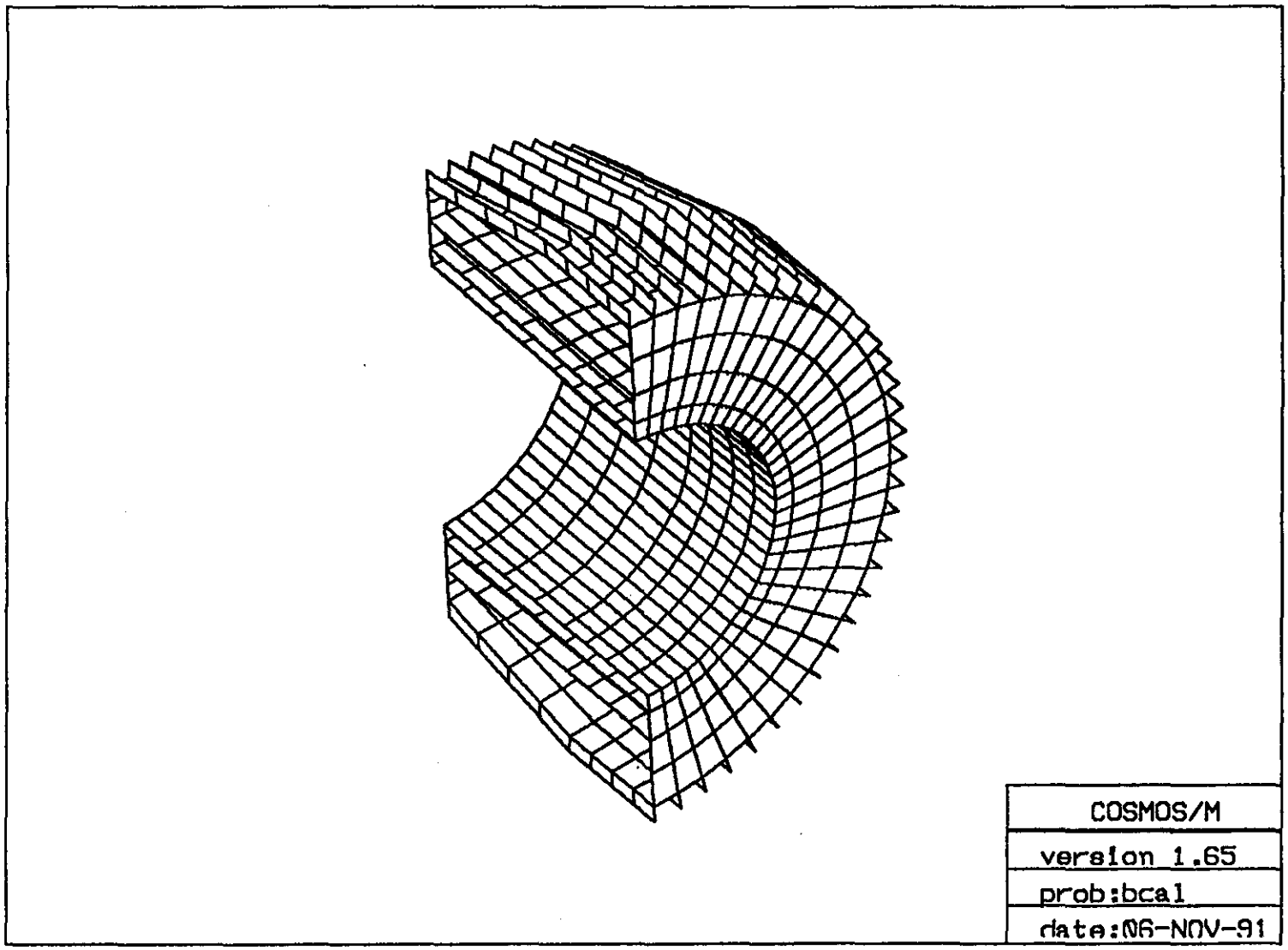

Figure 3

EM – HAC1 BOUNDARY
NORMAL FORCE

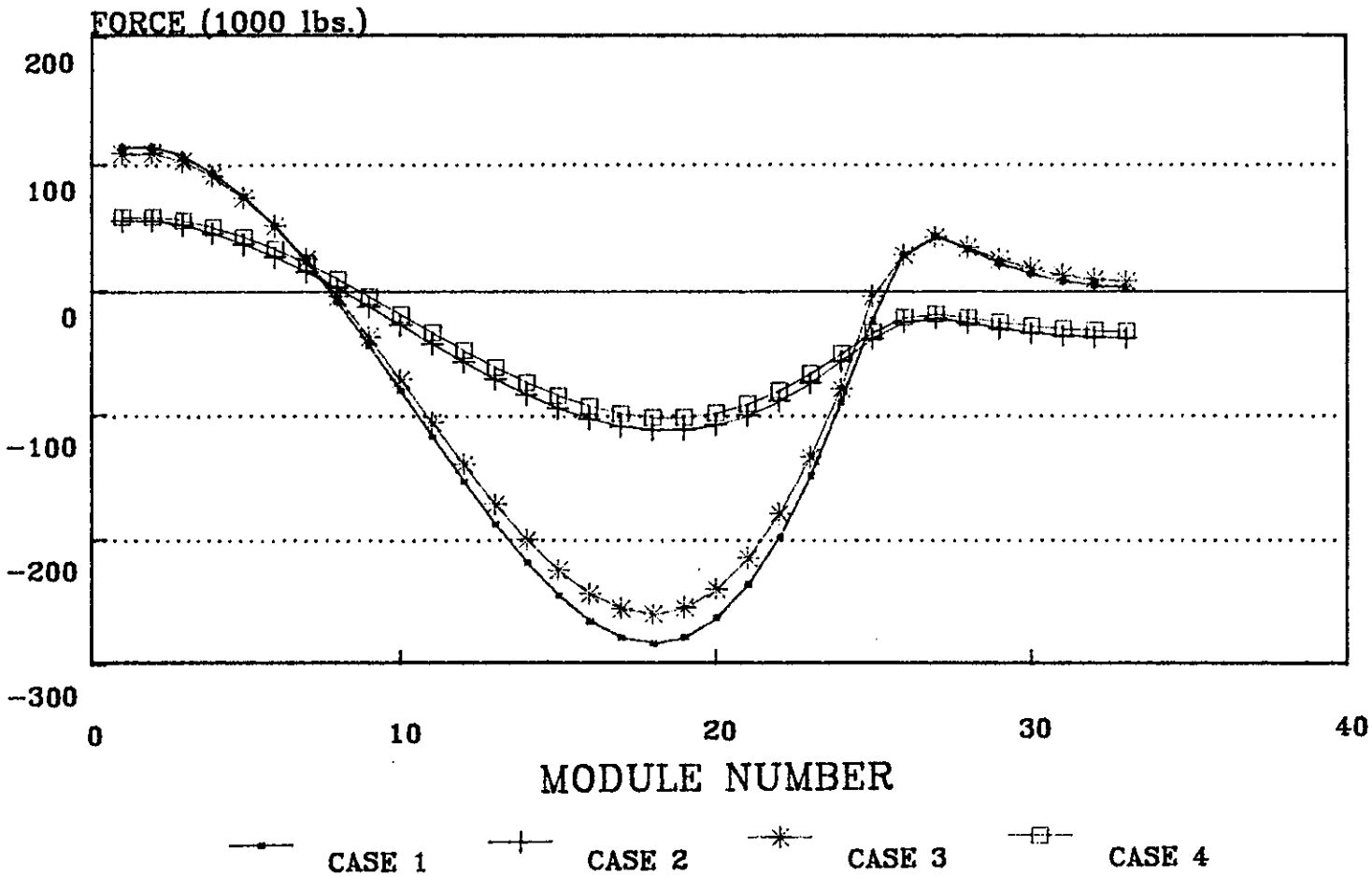

Figure 4

HAC1 — HAC2 BOUNDARY

NORMAL FORCE

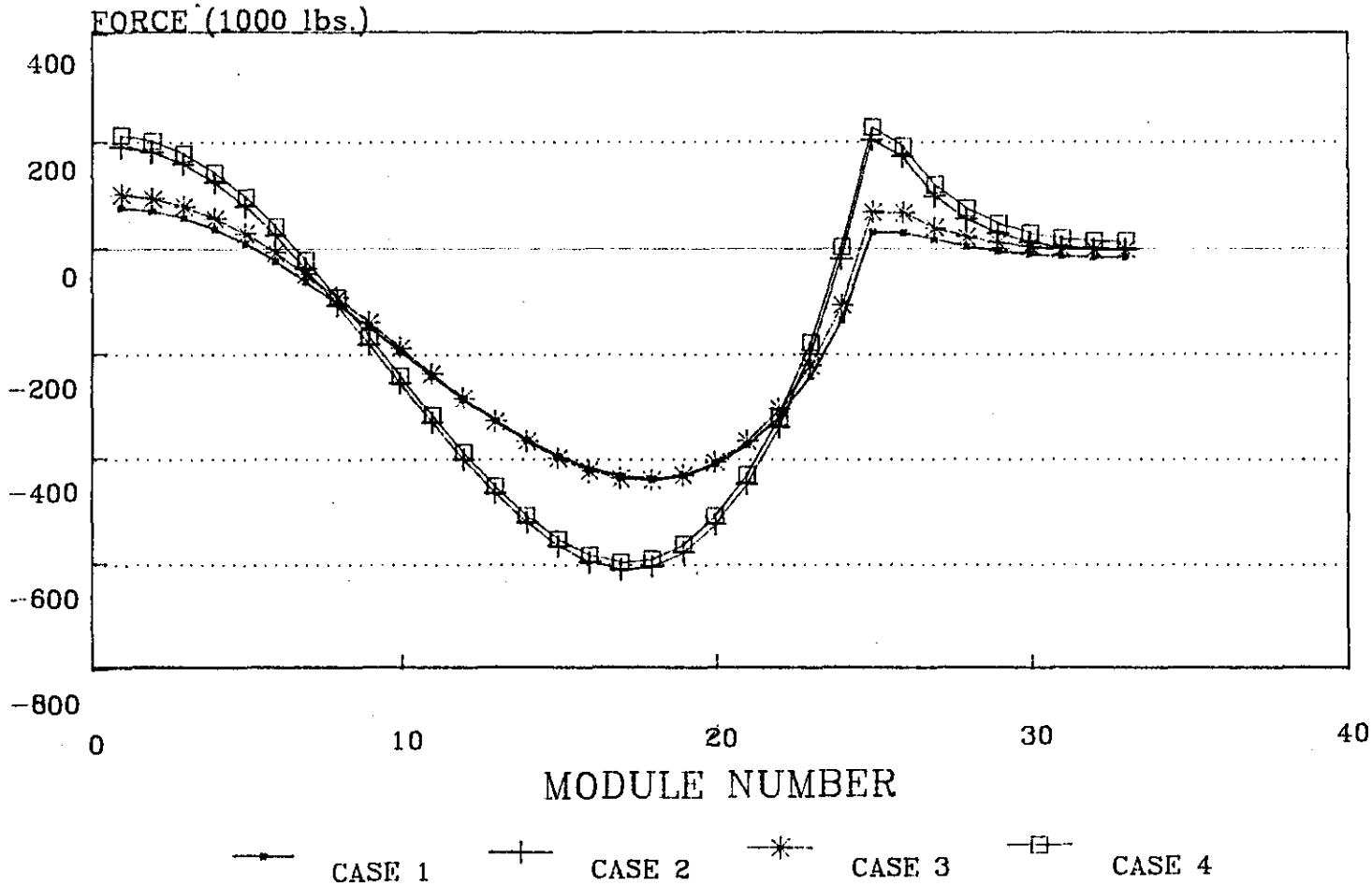

Figure 5

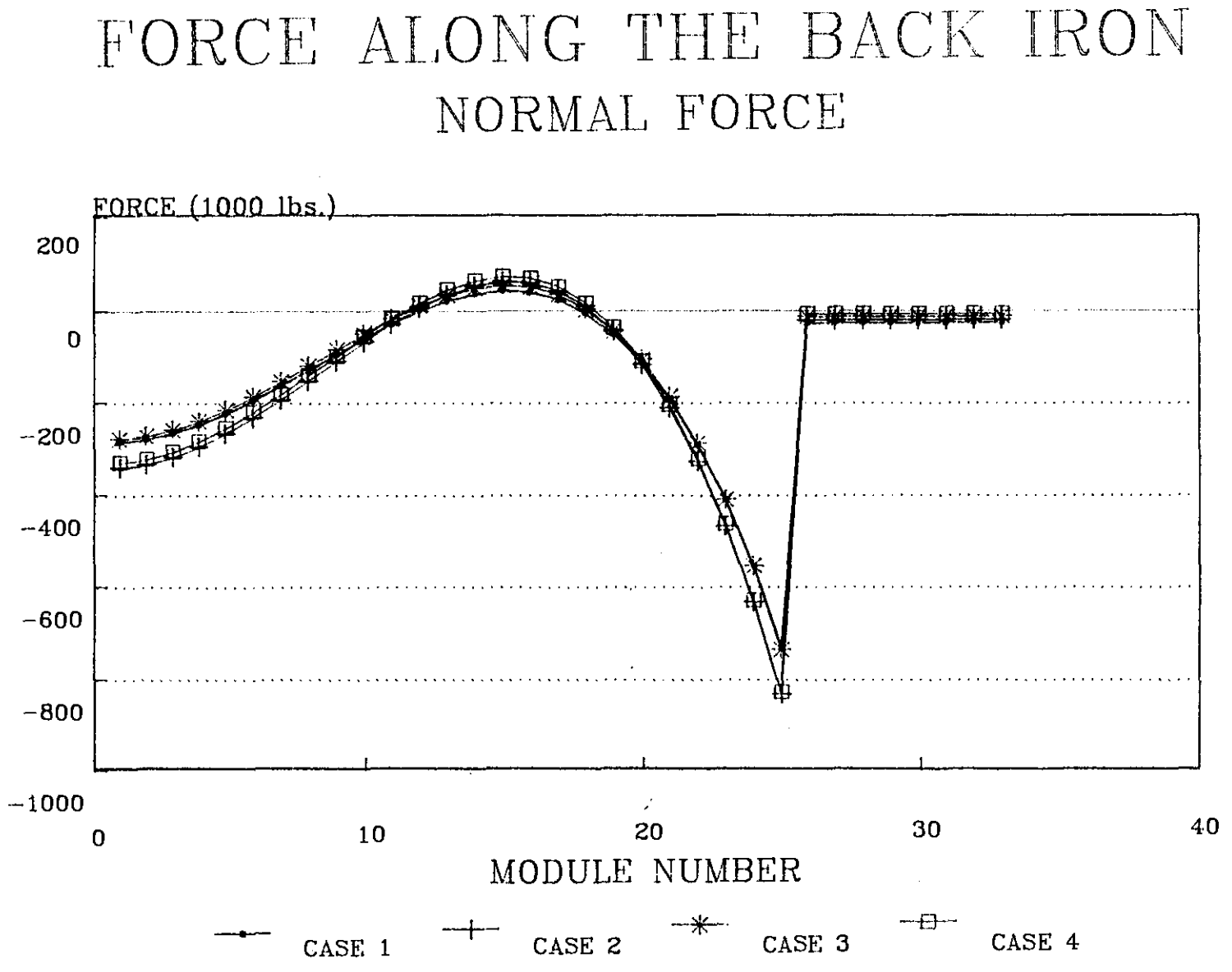
FORCE ALONG THE BACK IRON
NORMAL FORCE
FORCE (1000 lbs.)
200
0
-200
-400
-600
-800
-1000
0
10
20
30
40
MODULE NUMBER
CASE 1
CASE 2
CASE 3
CASE 4

Figure 6

EM – HAC1 BOUNDARY

RADIAL SHEAR FORCE

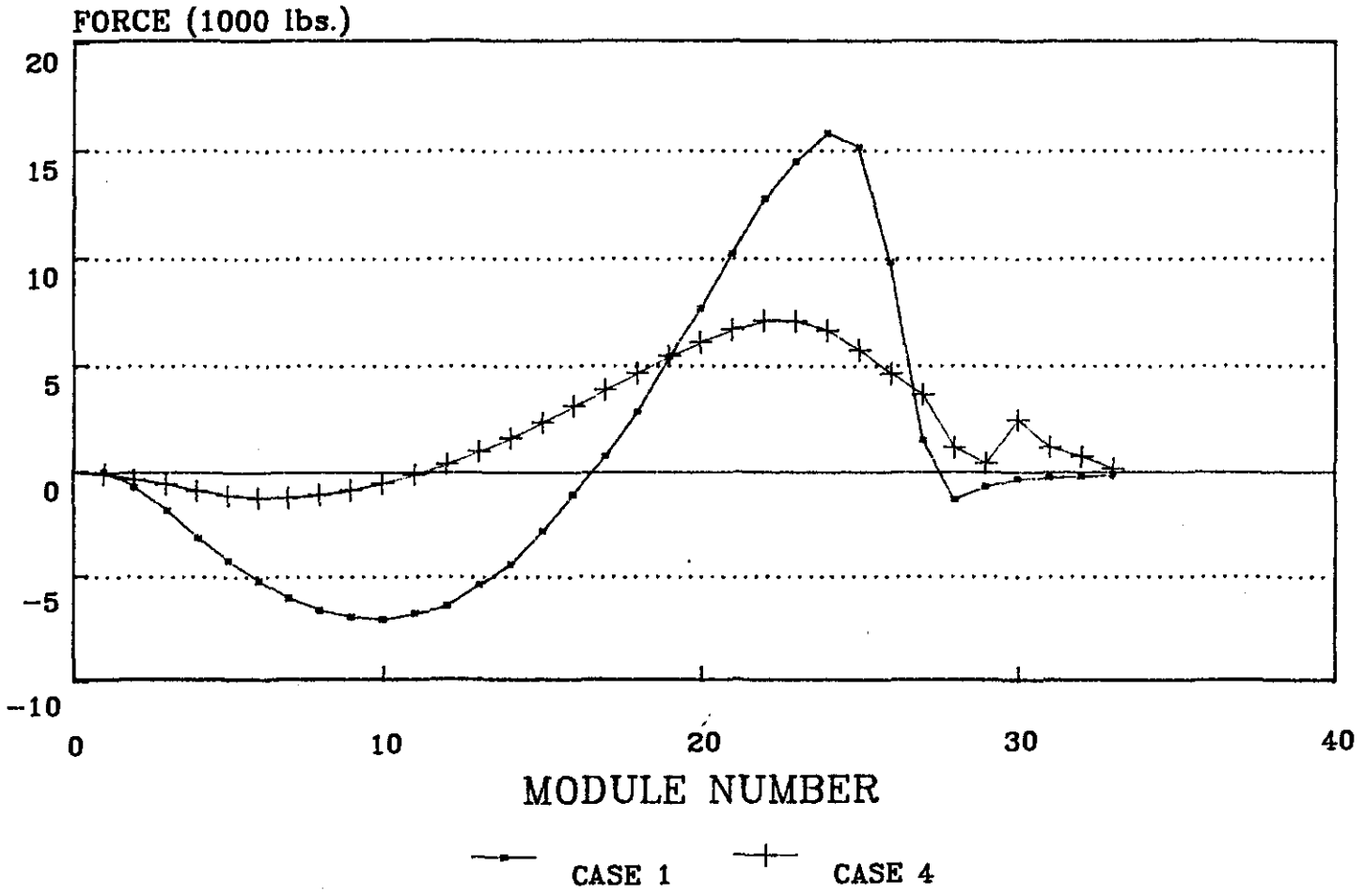

Figure 7

HAC1 – HAC2 BOUNDARY

RADIAL SHEAR FORCE

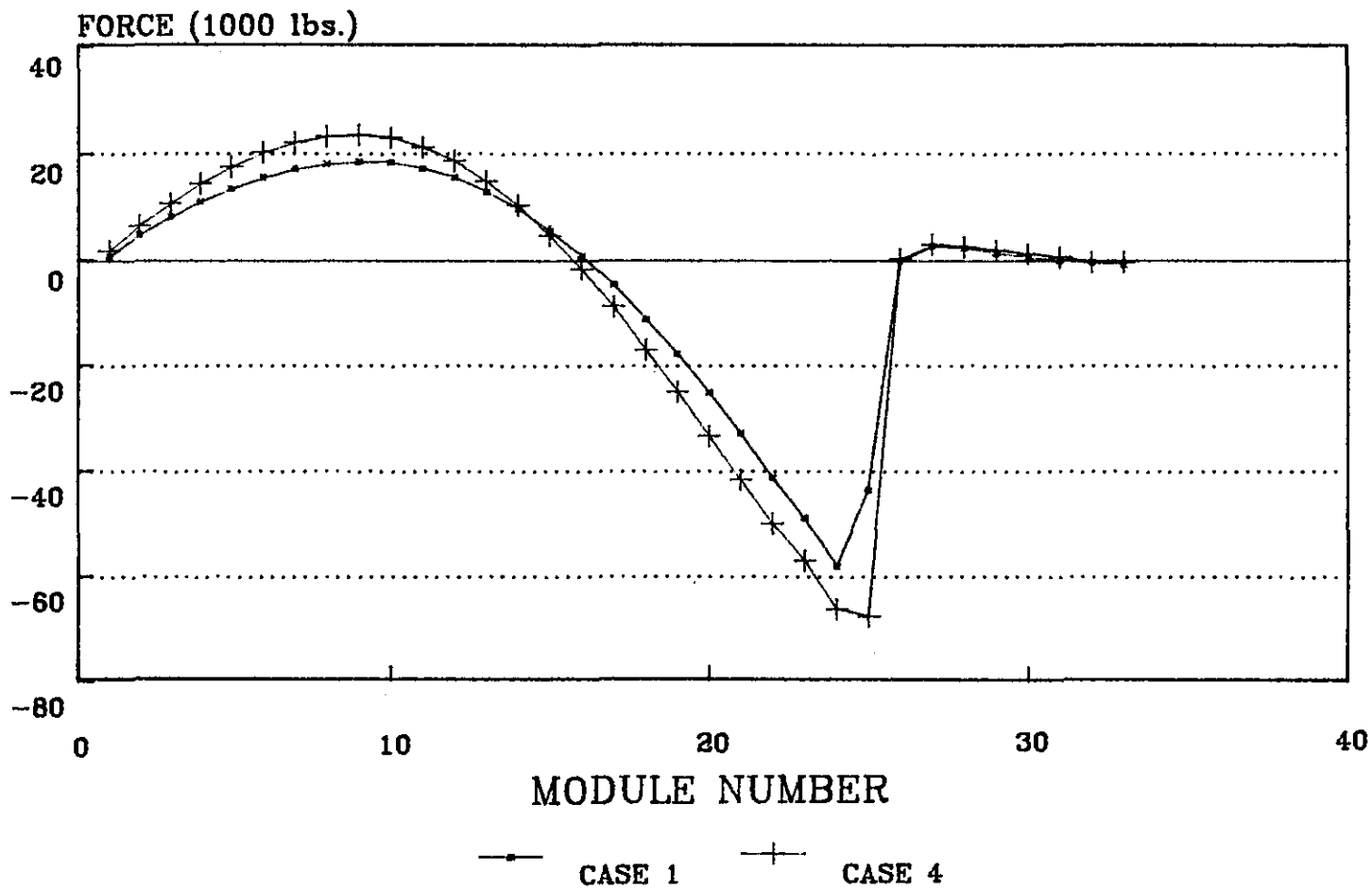

Figure 8

FORCE ALONG THE BACK IRON

RADIAL SHEAR

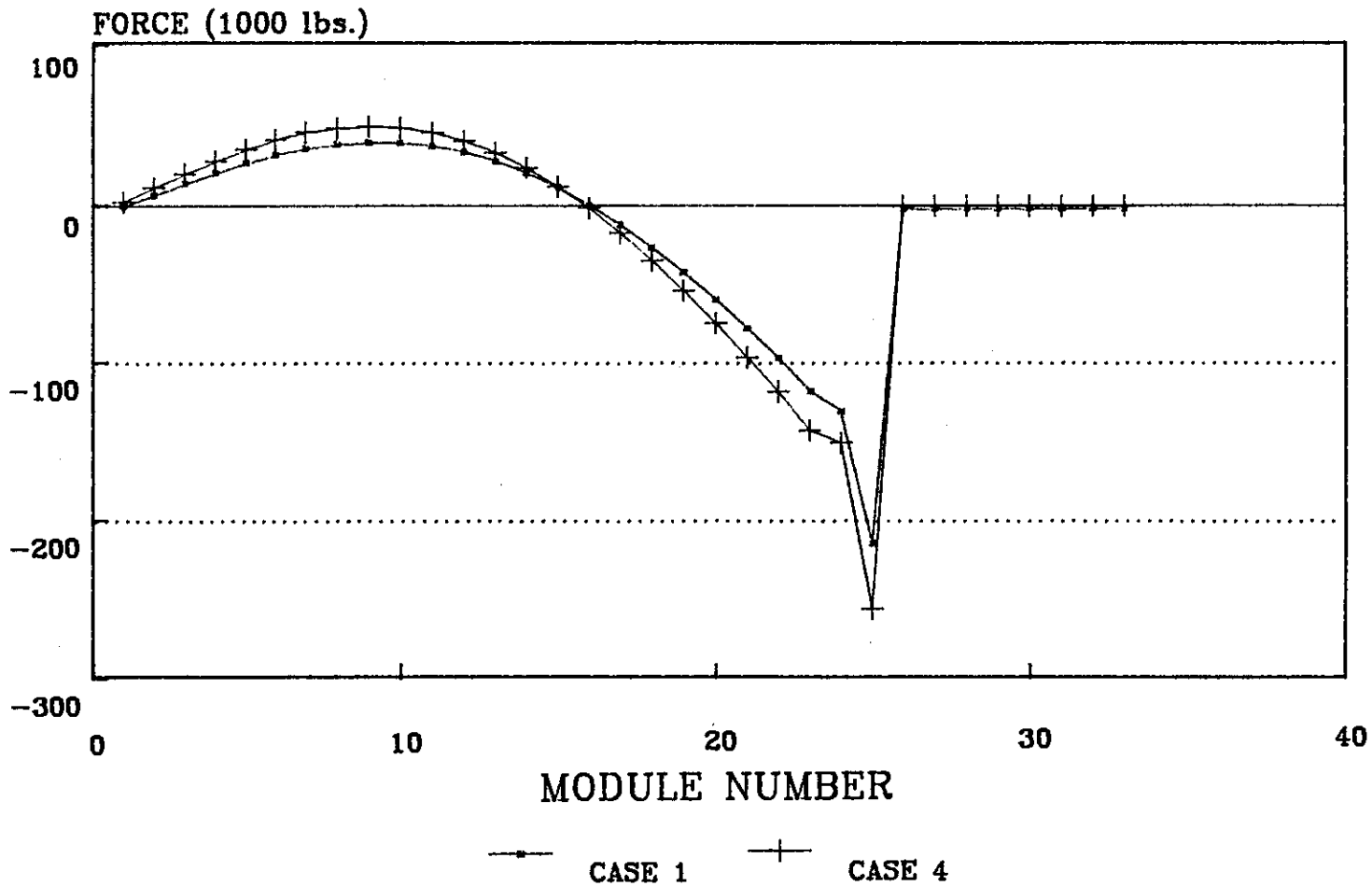

Figure 9

EM – HAC1 BOUNDARY

Z DIRECTION SHEAR

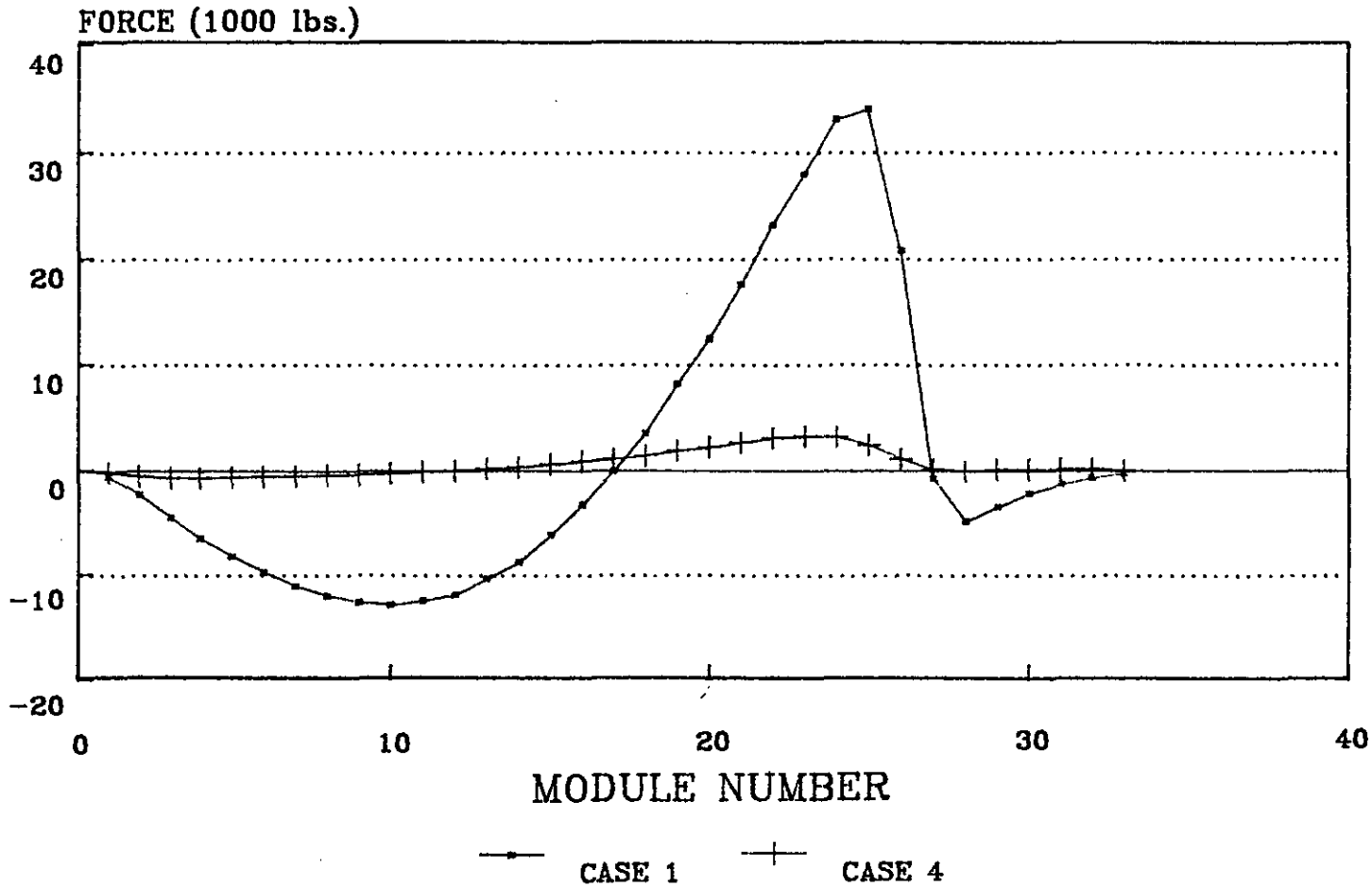

Figure 10

HAC1 – HAC2 BOUNDARY

Z DIRECTION SHEAR

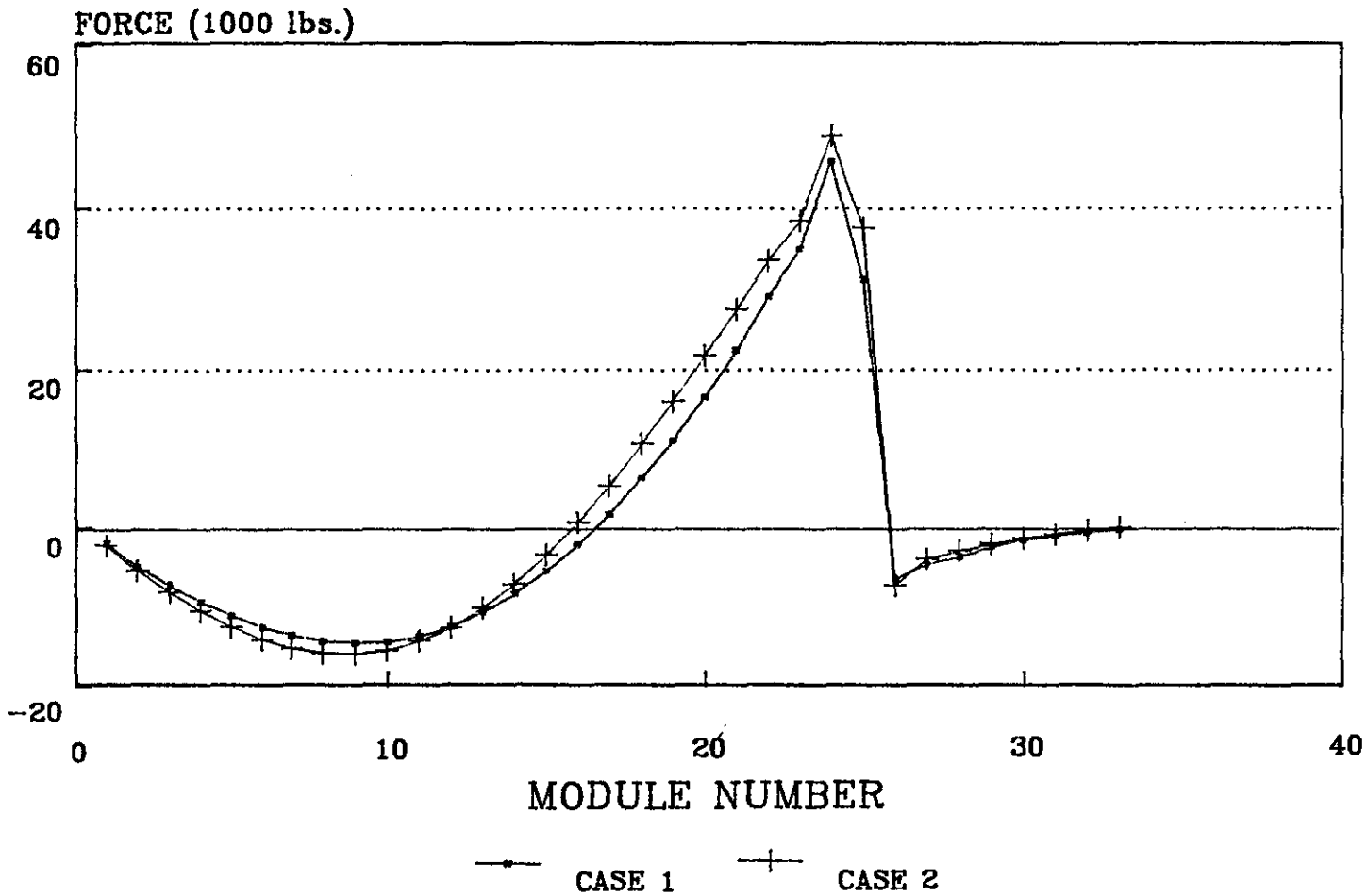

Figure 11

FORCE ALONG THE BACK IRON

Z DIRECTION SHEAR

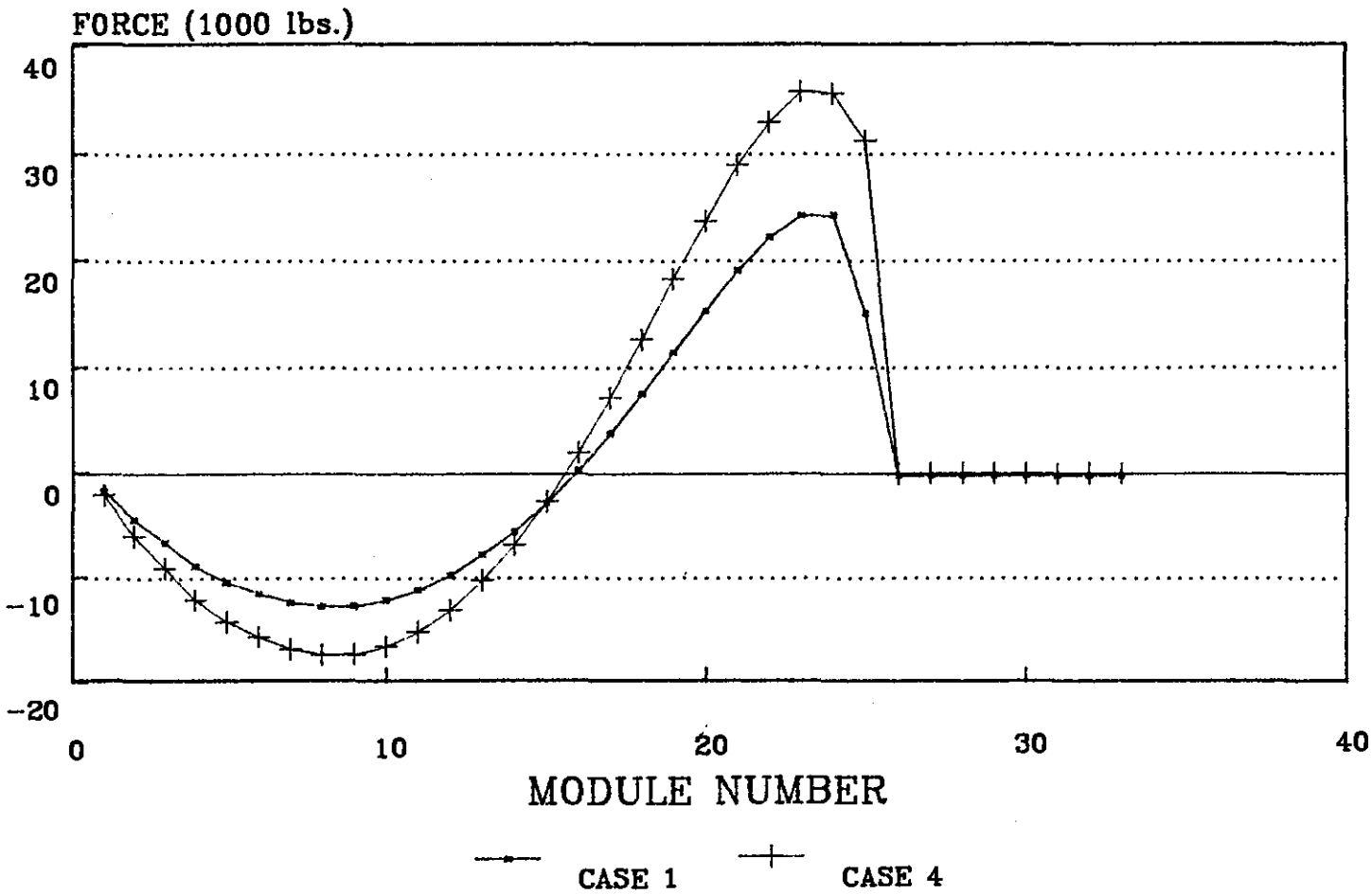

Figure 12

VERTICAL DEFLECTION
OUTSIDE DIAMETER

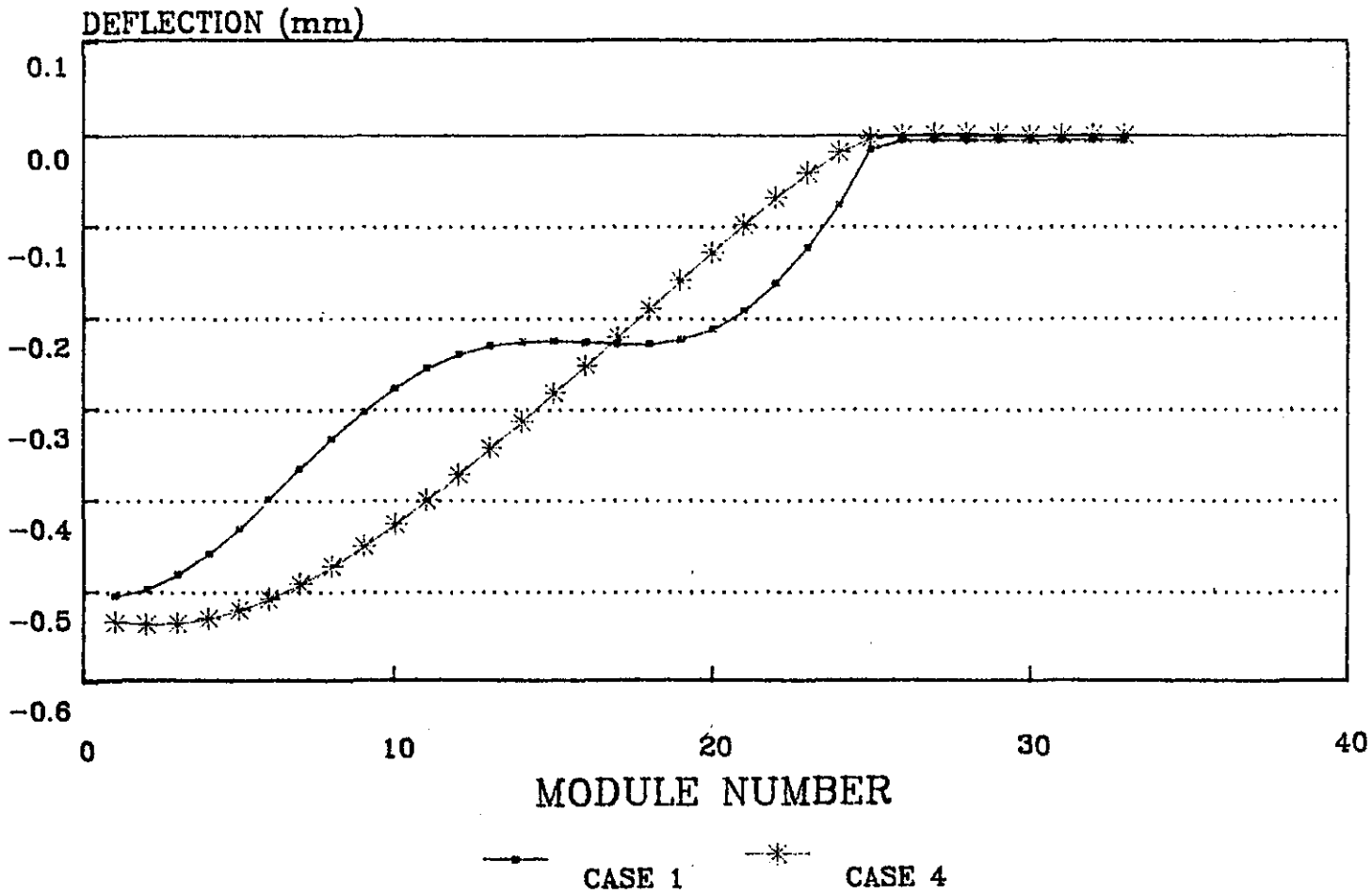

Figure 13

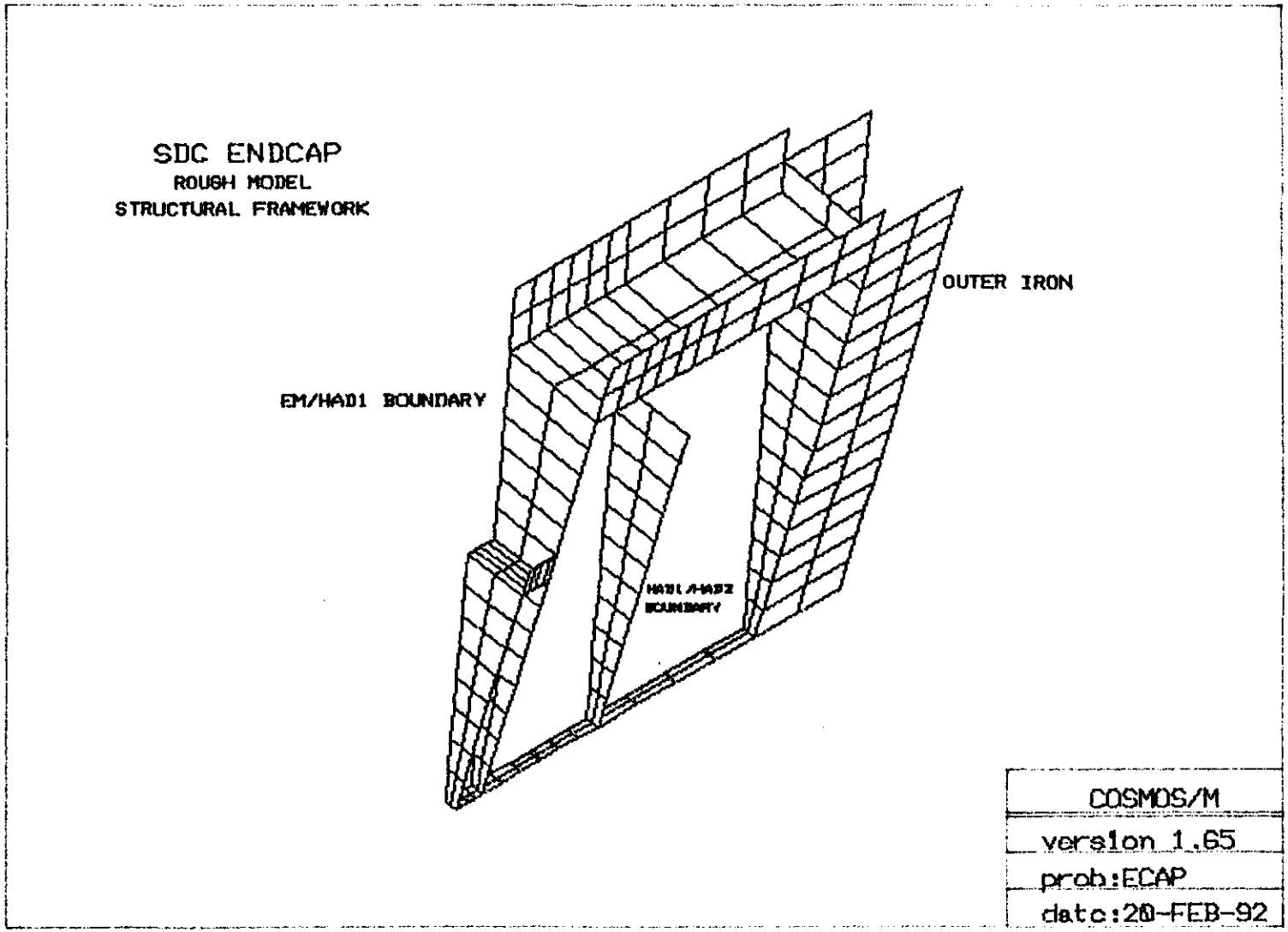
SDC ENDCAP
ROUGH MODEL
STRUCTURAL FRAMEWORK
OUTER IRON
EM/HAD1 BOUNDARY
COSMOS/M
version 1.65
prob:ECAP
date:20-FEB-92

Figure 14

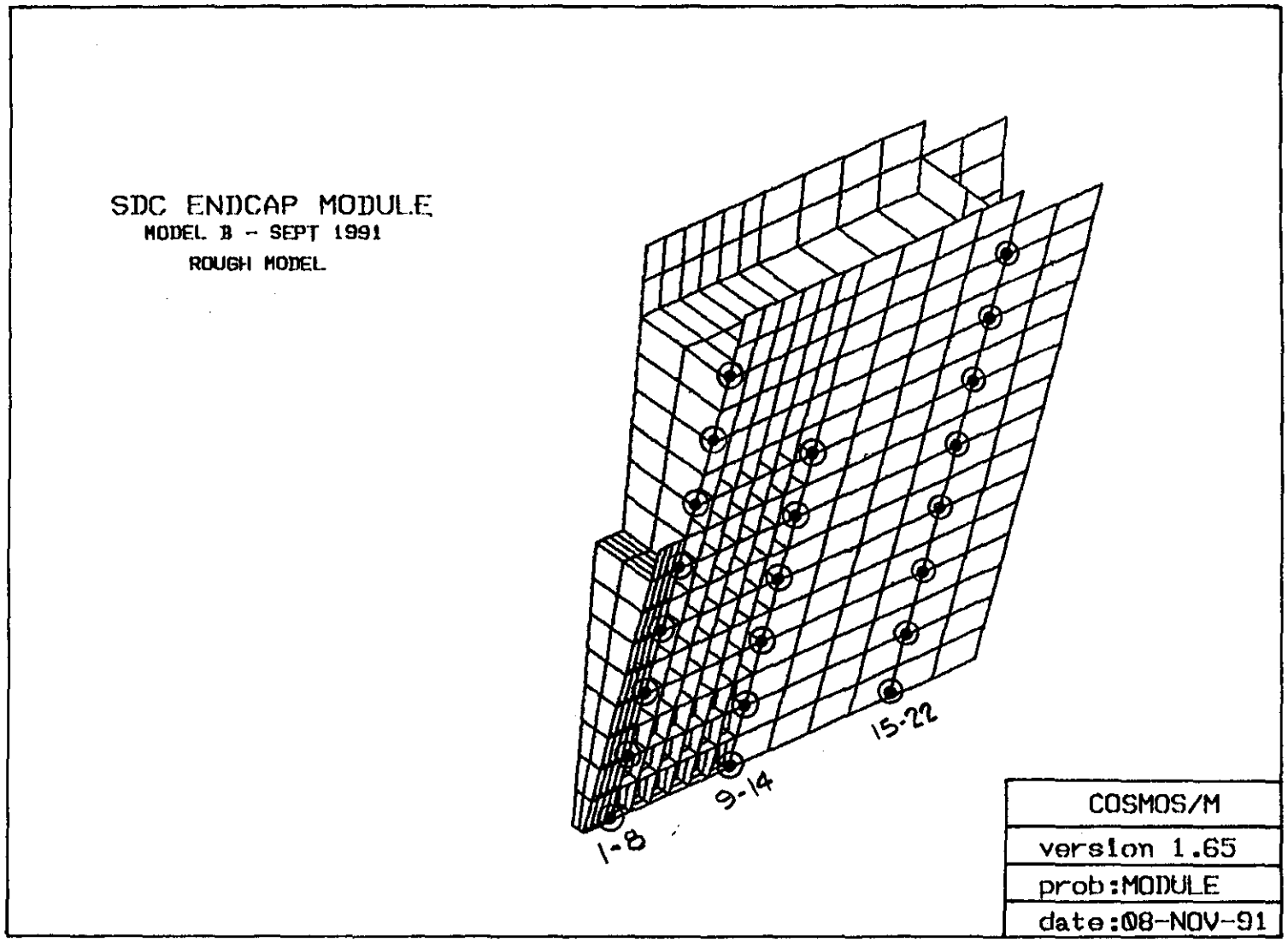
SDC ENDCAP MODULE
MODEL B - SEPT 1991
ROUGH MODEL
1-8
9-14
15-22
COSMOS/M
version 1.65
prob:MODULE
date:08-NOV-91

Figure 15

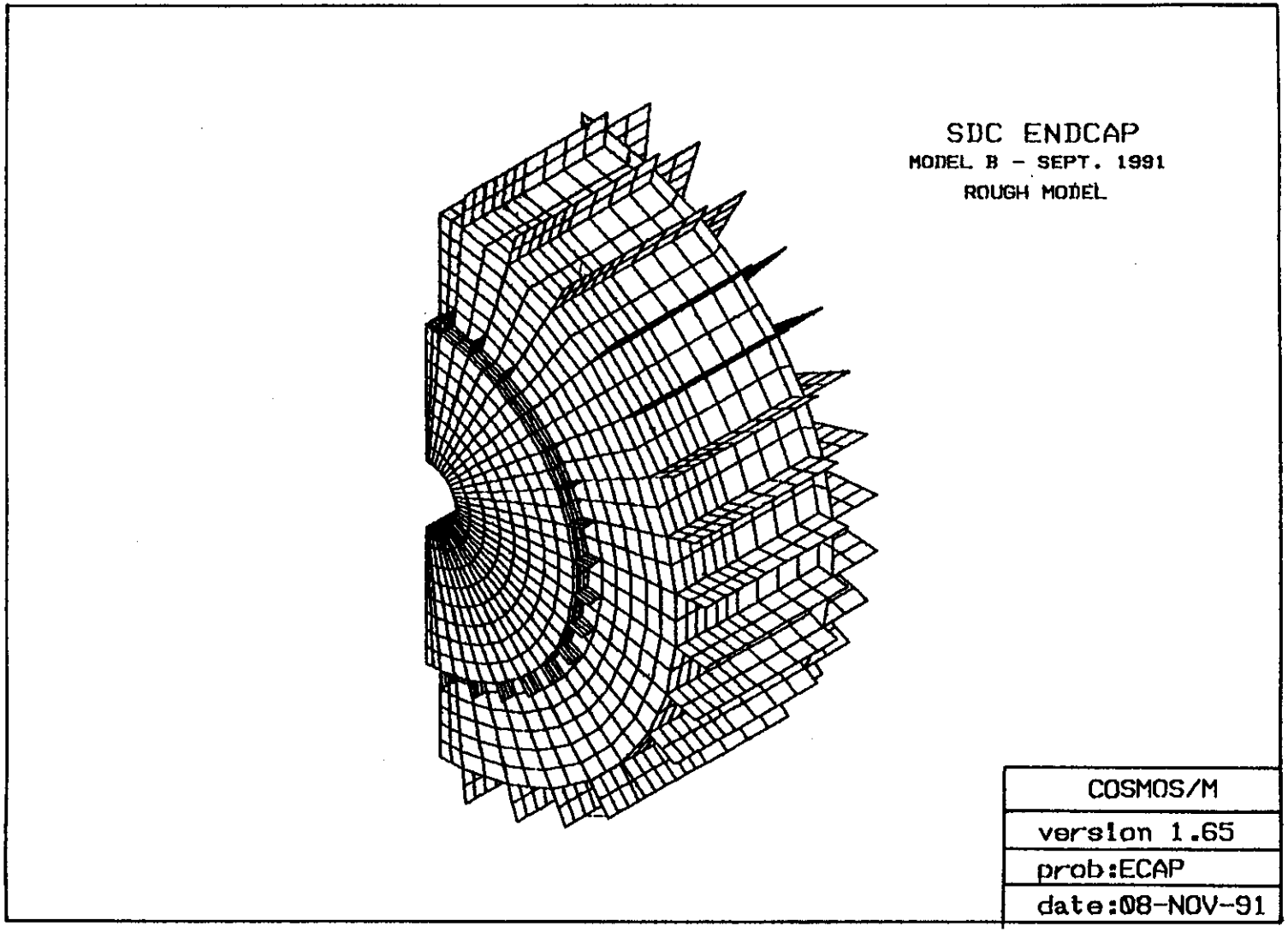
SDC ENDCAP
MODEL B - SEPT. 1991
ROUGH MODEL
COSMOS/M
version 1.65
prob:ECAP
date:08-NOV-91

Figure 16

EM/HAD1 Boundary
Normal Forces

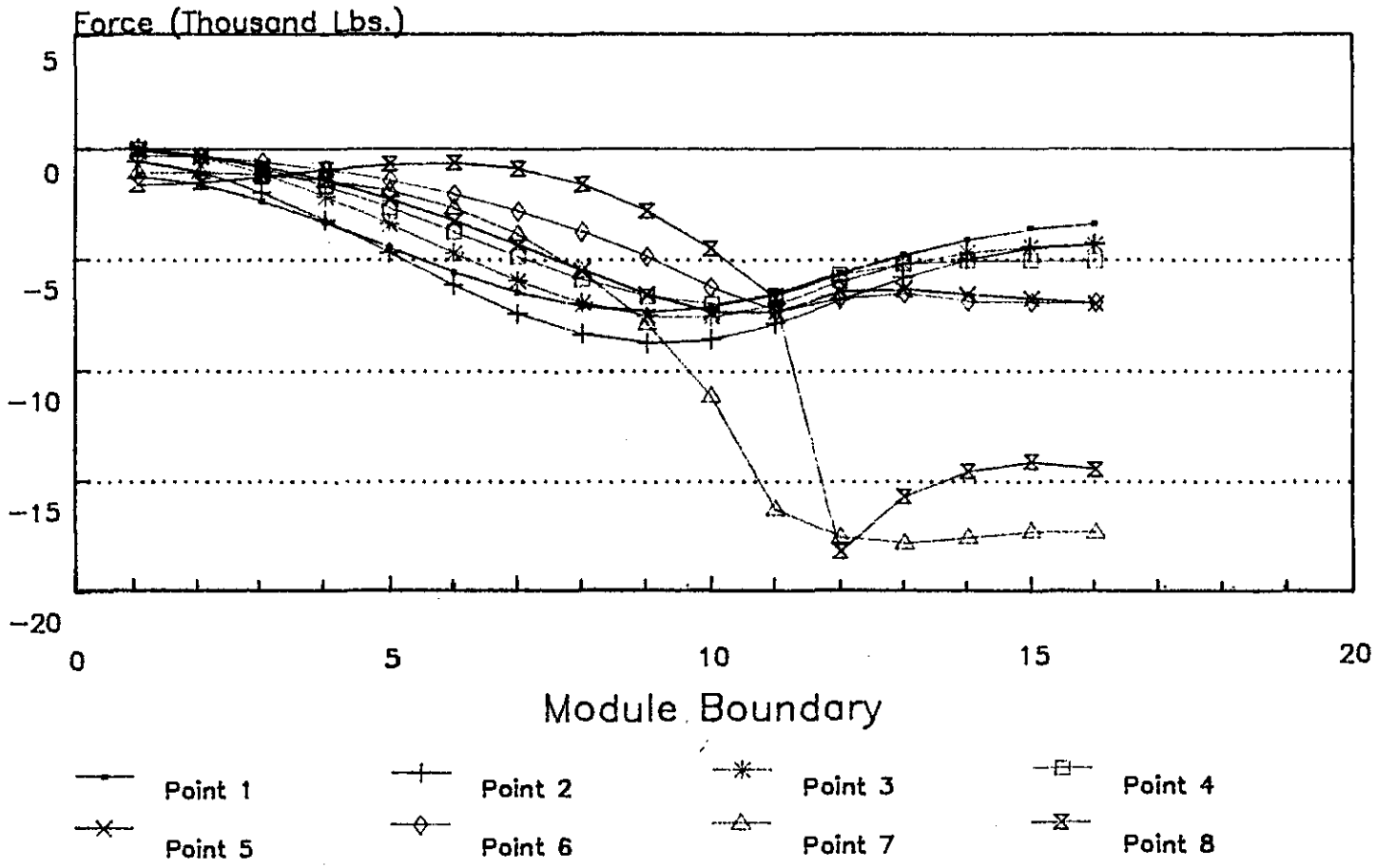

Pts. increase from ID to OD

Figure 17

HAD1/HAD2 Boundary

Normal Forces

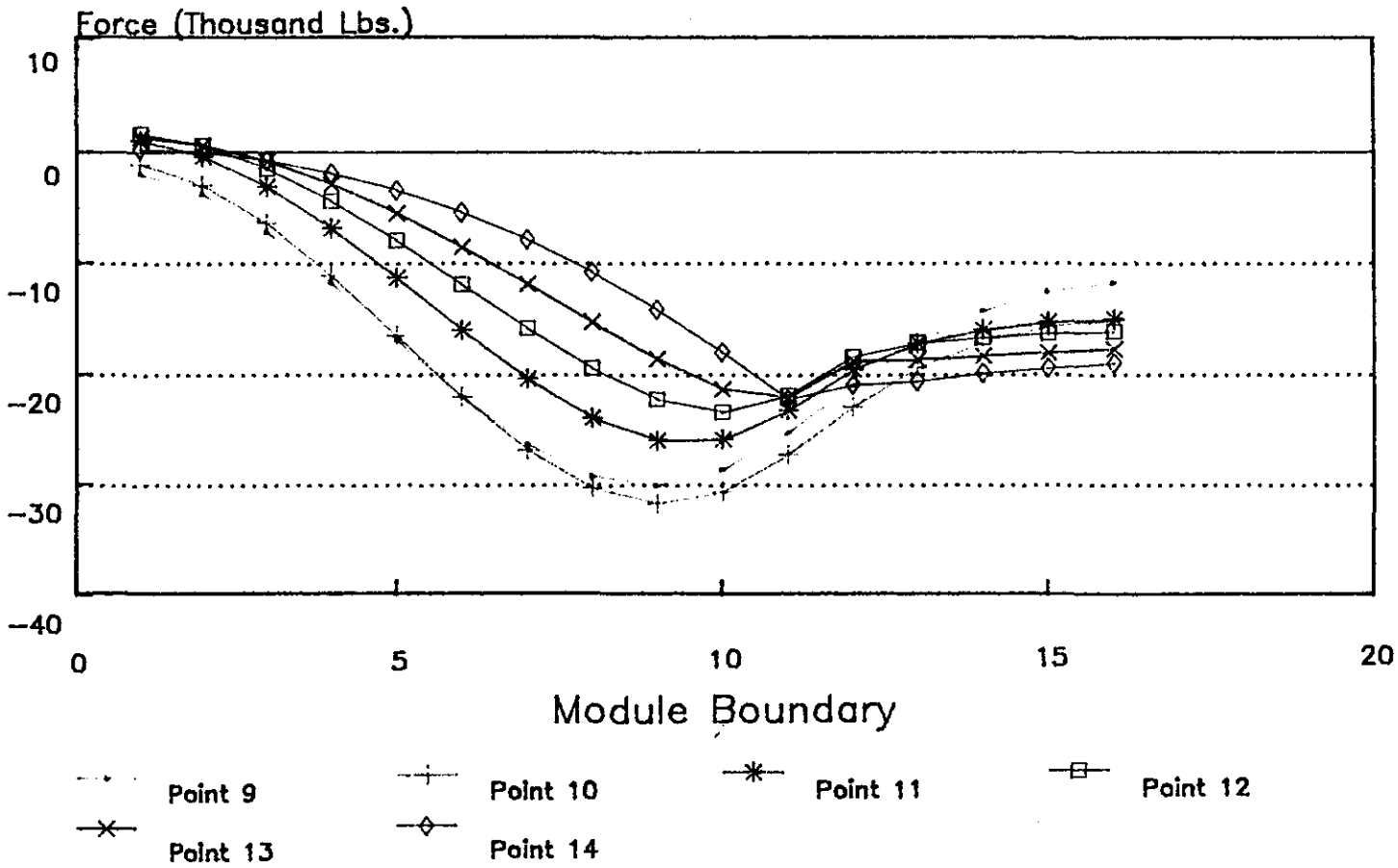

Points increase from ID to OD

Figure 18

Outer Iron Boundary

Normal Forces

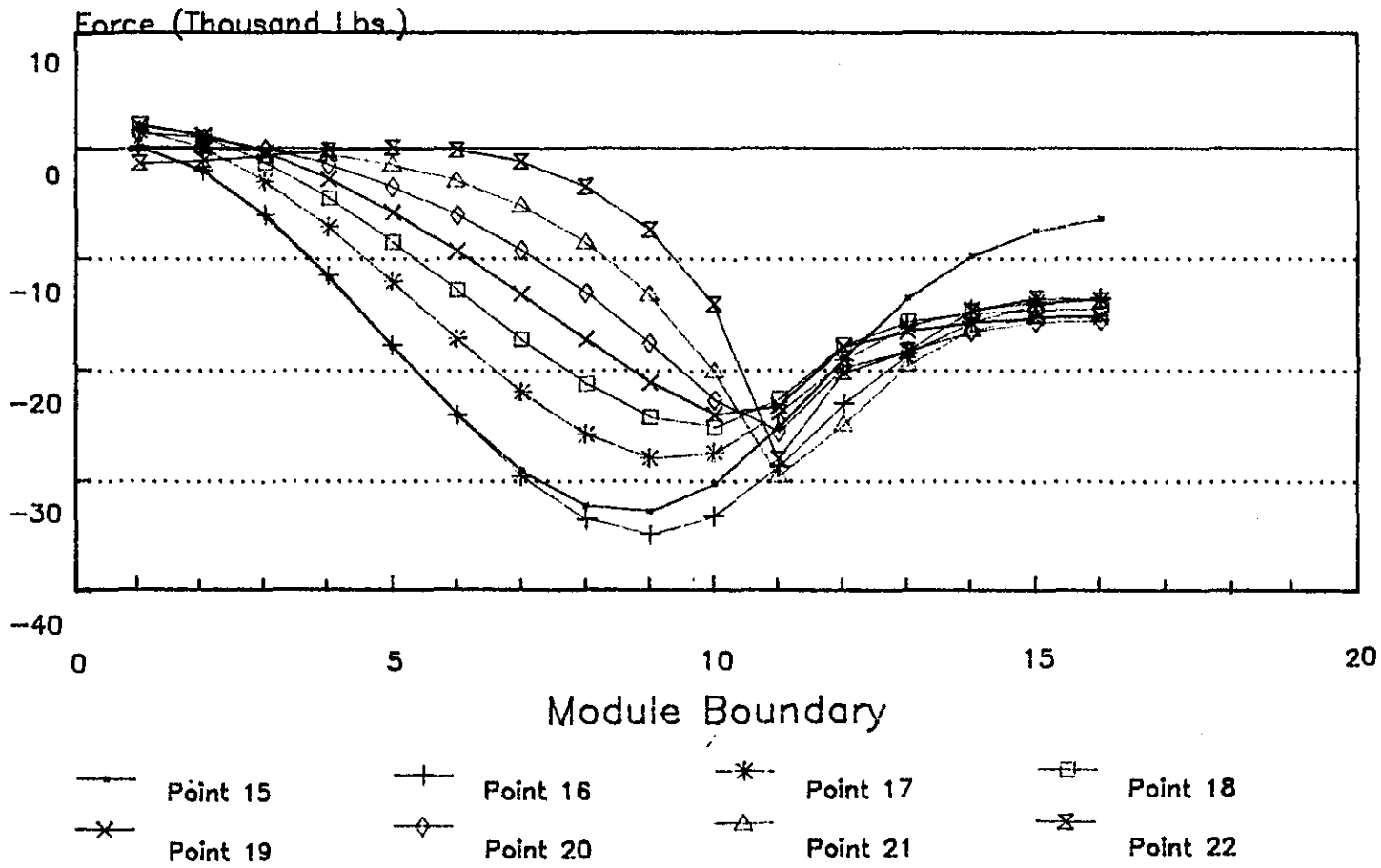

Points increase from ID to OD

Figure 19

EM/HAD1 Boundary

Radial Shear Forces

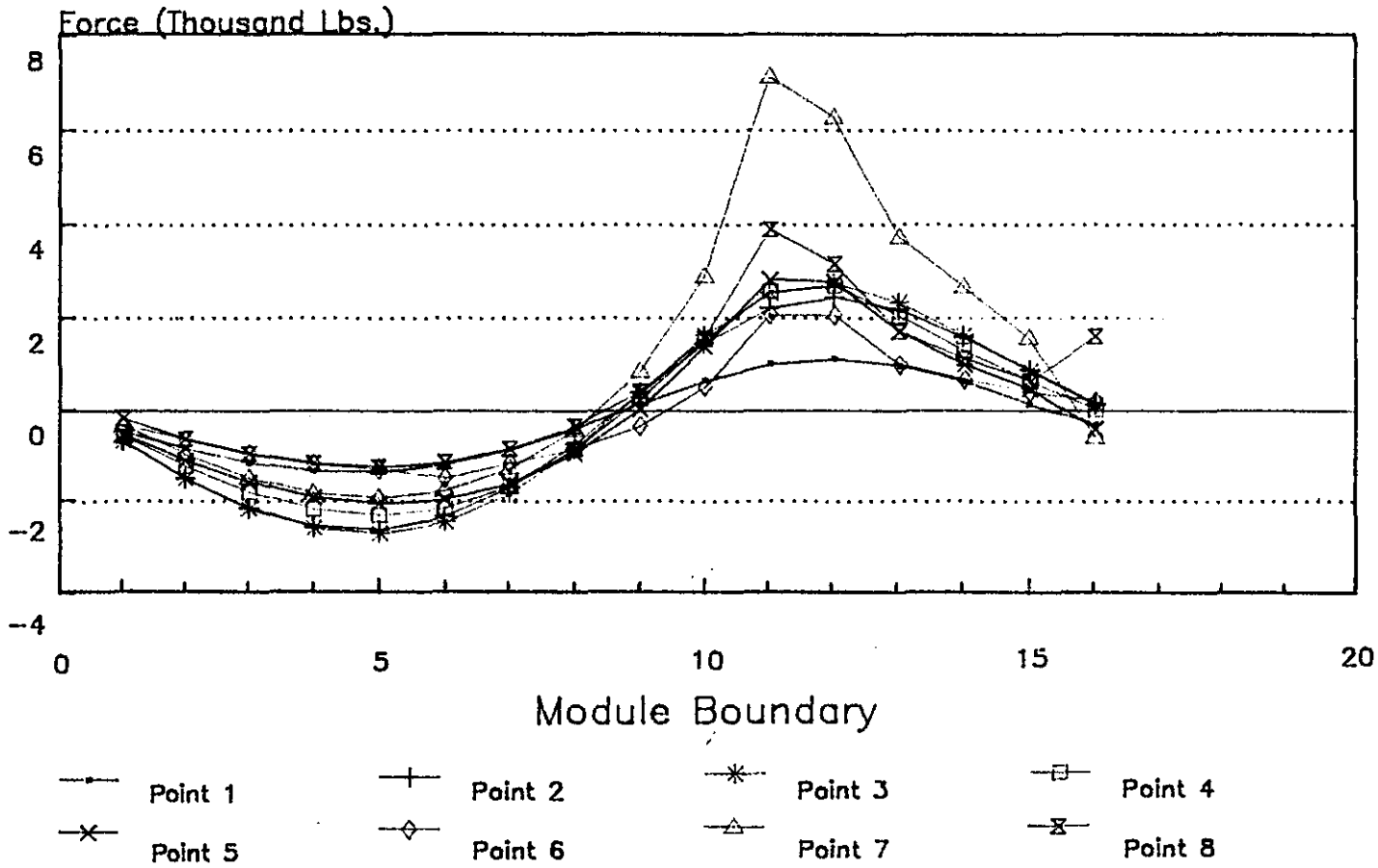

Points increase from ID to OD

Figure 20

HAD1/HAD2 Boundary

Radial Shear Forces

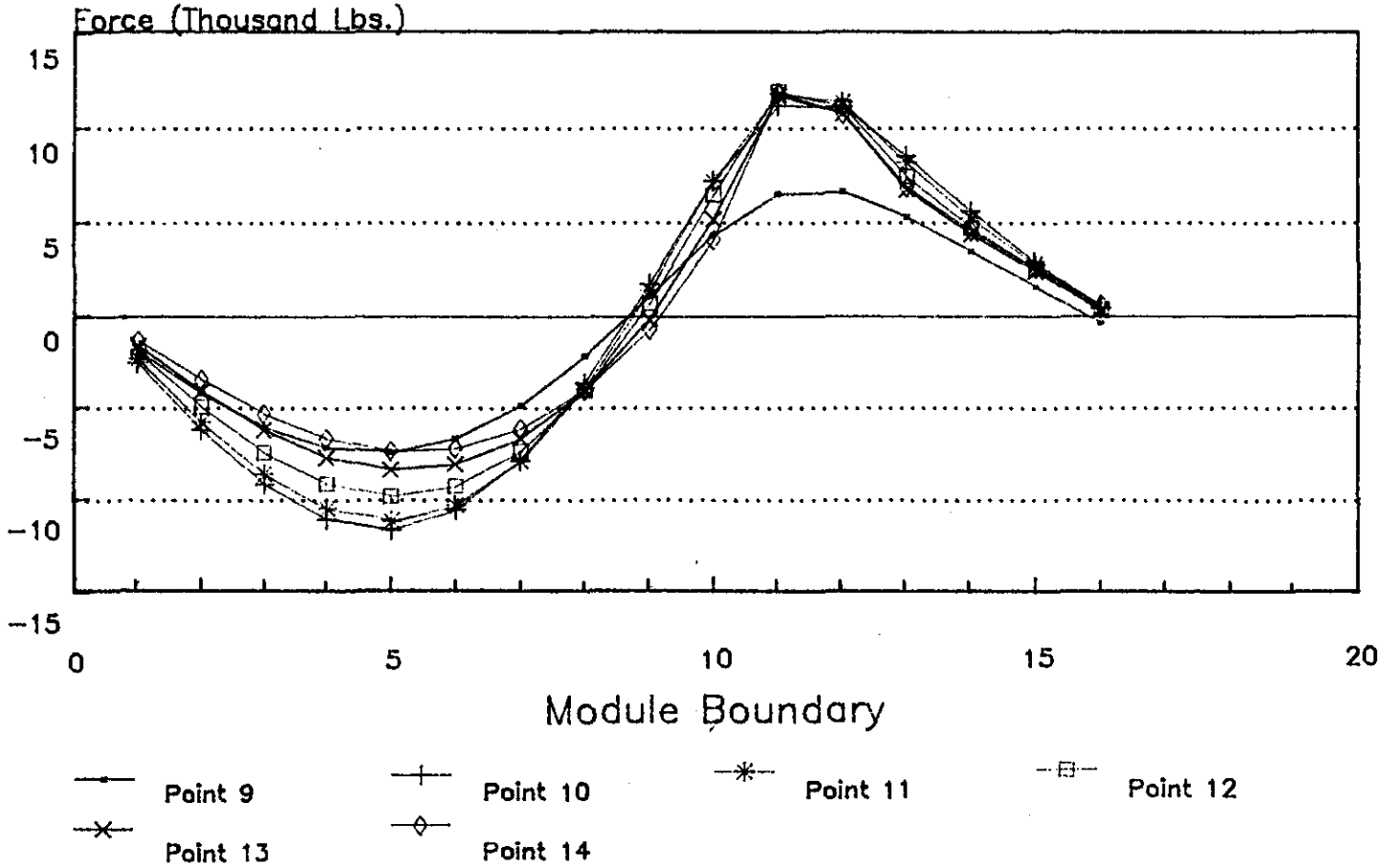

Points increase from ID to OD

Figure 21

Outer Iron Boundary

Radial Shear Forces

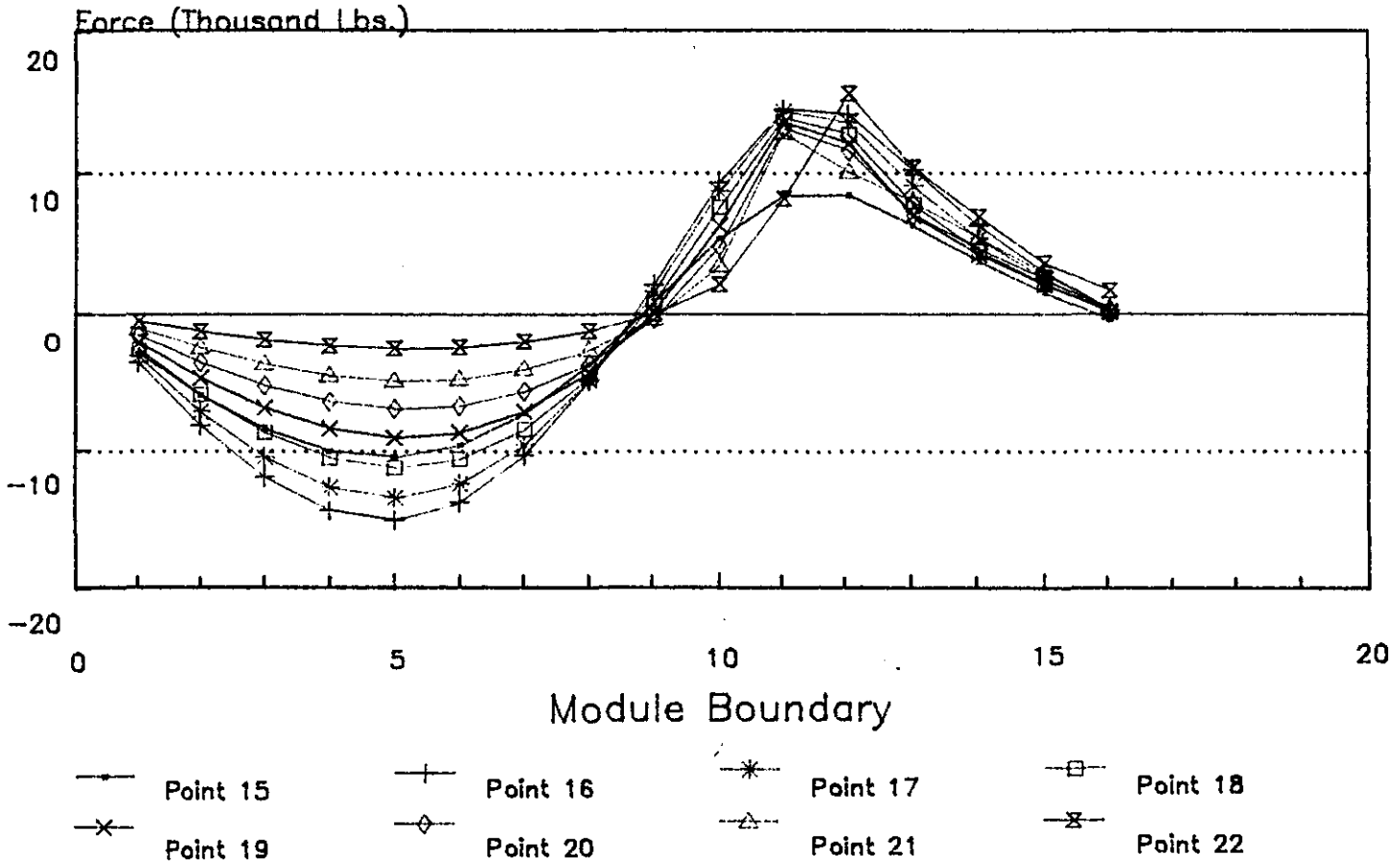

Points increase from ID to OD

Figure 22

EM/HAD1 Boundary

Z Direction Shear Forces

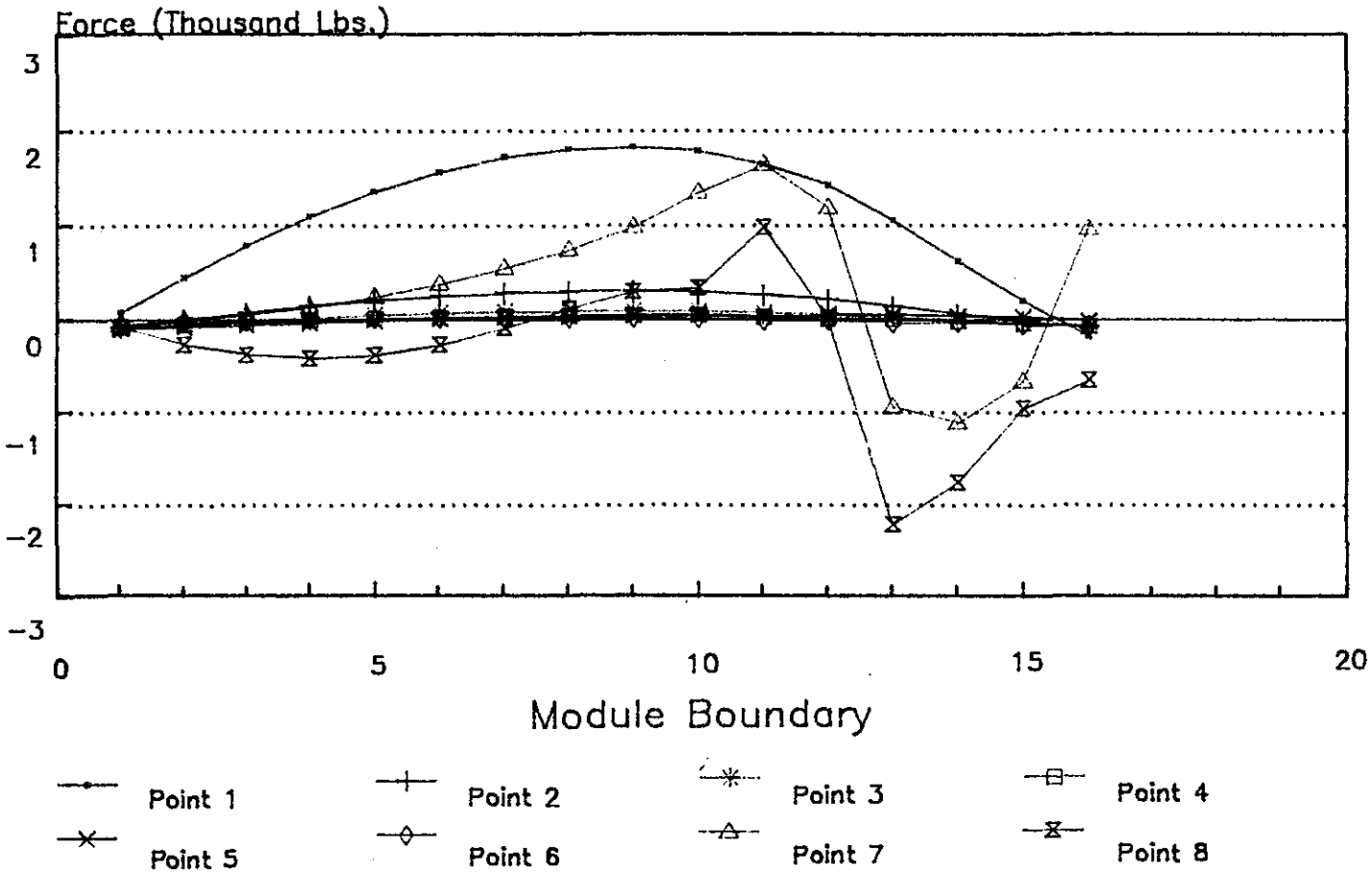

Points increase from ID to OD

Figure 23

HAD1/HAD2 Boundary

Z Direction Shear Forces

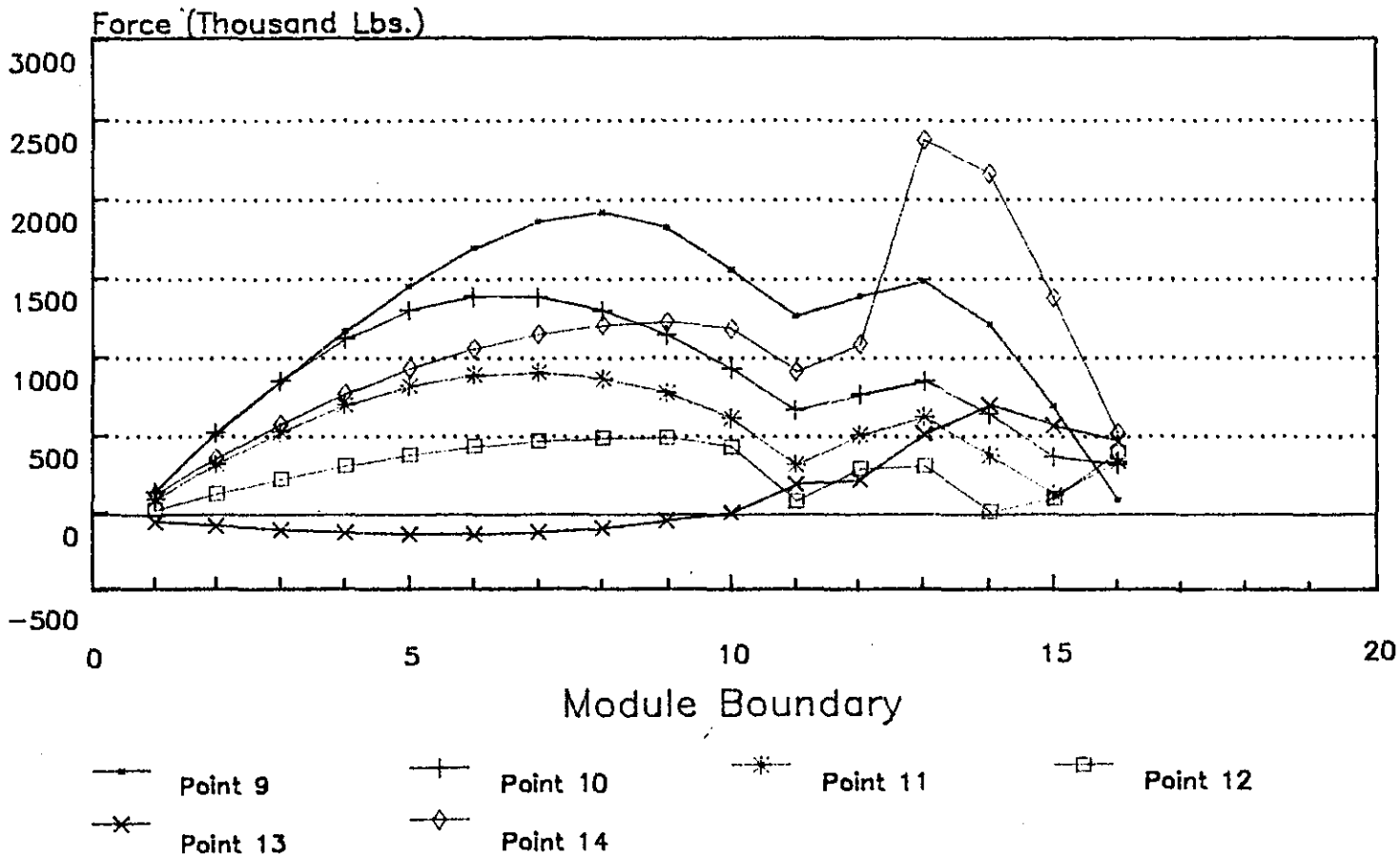

Points increase from ID to OD

Figure 24

Outer Iron Boundary

Z Direction Shear Forces

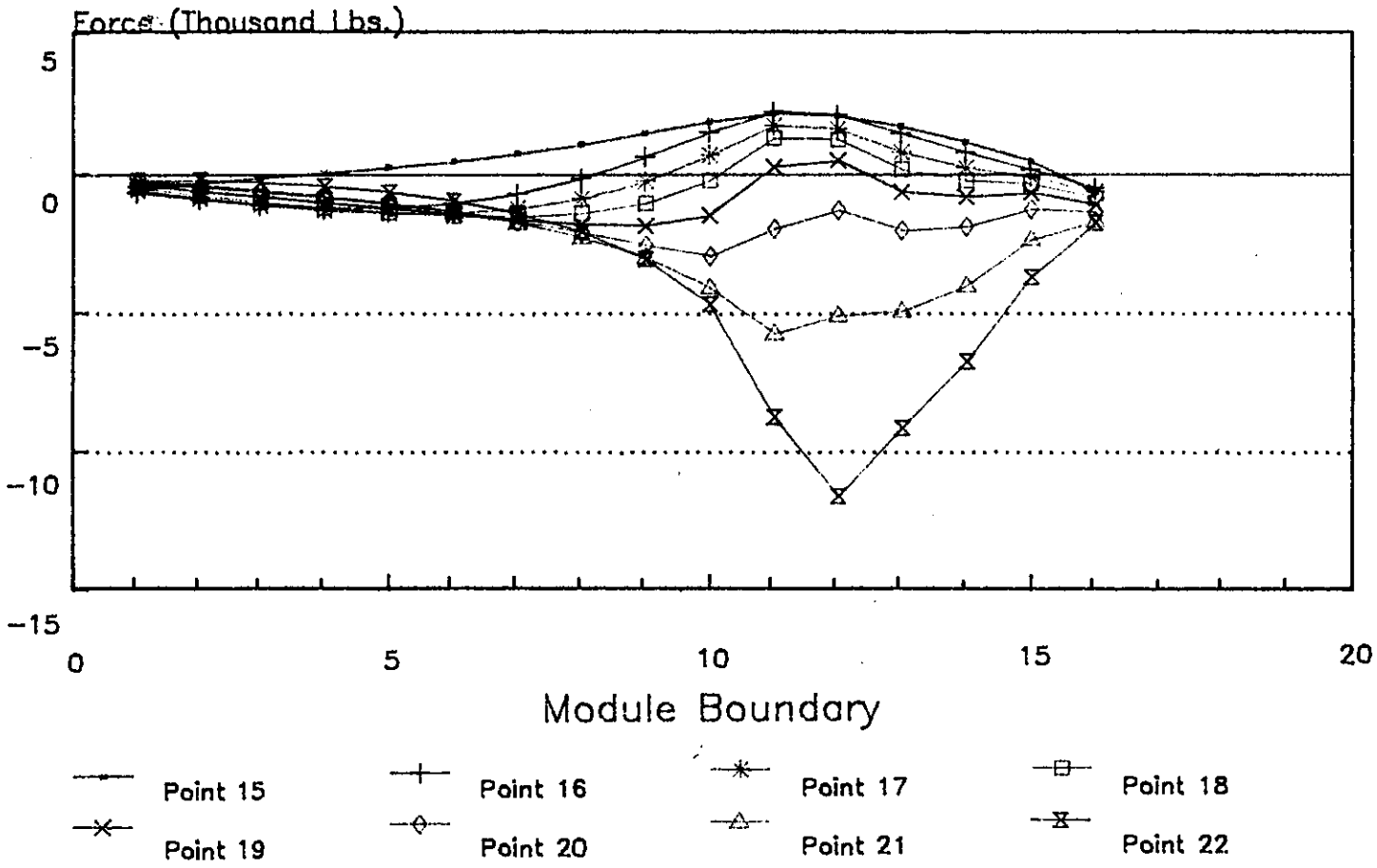

Points increase from ID to OD

Figure 25